

# Adsorption of Benzene on a Mo(112)–c(2 × 2)-[SiO<sub>4</sub>] Surface

M. S. Chen, A. K. Santra, and D. W. Goodman\*

Department of Chemistry, Texas A&M University, P.O. Box 30012, College Station, Texas 77842-3012

Received: May 21, 2004; In Final Form: August 13, 2004

The orientation and growth of benzene and pyridine on a well-ordered Mo(112)–c(2 × 2)-[SiO<sub>4</sub>] have been investigated with high-resolution electron energy loss spectroscopy (HREELS), Auger spectroscopy (AES) and low-energy electron diffraction (LEED). Benzene on the c(2 × 2)-[SiO<sub>4</sub>] surface is bound with its molecular plane parallel to the surface plane at submonolayer coverages. At intermediate coverages (1–3 ML), in contrast to benzene adsorption on metal surfaces, a layer-by-layer growth mode is observed with the benzene molecules bonded parallel to the surface. Pyridine on the c(2 × 2)-[SiO<sub>4</sub>] surface, on the other hand, undergoes a phase transition from a parallel to a tilted configuration. This is the first reported observation of benzene multilayer growth in which the benzene molecules bond exclusively parallel to the surface plane. The origin for this unusual adsorption behavior of benzene is discussed.

## 1. Introduction

Benzene is an ideal adsorbate for studying anisotropic molecule–surface and molecule–molecule interactions at surfaces. In the crystalline phase, benzene forms an orthorhombic lattice in which all four molecules in the unit cell arrange in a T configuration.<sup>1</sup> Bonding is via the  $\pi$  electrons of the aromatic ring that is oriented parallel to the surface plane<sup>2–5</sup> for most transition metal surfaces, with the exception of Pd(110)<sup>6,7</sup> and W(112).<sup>8</sup> In heterogeneous catalysis oxides are frequently used to support metal particles,<sup>9–12</sup> therefore understanding the interaction of various reactants with metal oxide surfaces is of fundamental importance. In contrast to the abundance of studies of benzene adsorption on metal surfaces, there are very few studies of the adsorption of benzene on well-defined oxide surfaces.<sup>13–18</sup> Problems of surface charging with many surface analytical probes has limited studies on insulating surfaces of oxides, with most such studies carried out on semiconducting surfaces, for example, TiO<sub>2</sub><sup>14–16</sup> and ZnO.<sup>17,18</sup> The consensus is that benzene adsorbs with its plane parallel to the oxide surface, presumably  $\pi$ -bonding to the surface cations. Recently, thin, well-ordered oxide films have been successfully synthesized on metal surfaces<sup>19–22</sup> and used as models for the corresponding terminated bulk oxides. In particular, high-resolution electron energy loss spectroscopy (HREELS) has proved to be a powerful technique for investigating these model oxide systems.

In the present study, benzene adsorption on a well-ordered Mo(112)–c(2 × 2)-[SiO<sub>4</sub>] surface is investigated. The c(2 × 2)-[SiO<sub>4</sub>] surface (Figure 1) has been shown to be O-terminated using HREELS.<sup>23</sup> Briefly, only a single phonon feature corresponding to the Si–O asymmetry stretching mode appears at 131 meV in the HREEL spectrum, much too low in energy to be assigned to the Si–O–Si asymmetry stretching mode typically found at 147 meV for thick SiO<sub>2</sub> films. Because the film thickness was estimated to be 1 ML from AES, the 131 meV feature is assigned to a Si–O–Mo species, corresponding to an asymmetry stretching band for the Si–O–Mo species 15

meV lower than that for a Si–O–Si species.<sup>24–26</sup> In this oxide layer, all oxygen atoms in the [SiO<sub>4</sub>] tetrahedral are bound to the substrate Mo atoms, with the outmost layer oxygen atoms arranged in a quasi-hexagonal fashion as shown in Figure 1. For comparative purposes, pyridine adsorption on the c(2 × 2)-[SiO<sub>4</sub>] surface is also investigated.

## 2. Experimental Section

The experiments were carried out in an UHV chamber with a base pressure of  $<3 \times 10^{-10}$  Torr and equipped with high-resolution electron energy loss spectroscopy (HREELS, LK-2000), low-energy electron diffraction (LEED), a single-pass cylindrical mirror analyzer (CMA) for Auger electron spectroscopy (AES), and a UTI quadrupole mass spectrometry (QMS).

The Mo(112) sample was cleaned by repeated cycles of oxidation at 1200 K followed by a flash to 2100–2200 K and characterized using AES and LEED. The substrate temperature was measured via a (W/5 wt % Re)/(W/26 wt % Re) thermocouple spot-welded to the back sample surface. A liquid-nitrogen cryostat and an electron beam heater allowed control of the sample temperature between 90 and 2300 K. The silica films were prepared by evaporating Si onto the Mo(112) surface from a tantalum filament in UHV at room temperature; the details are described elsewhere.<sup>23</sup> Briefly, the Mo(112)–c(2 × 2)-[SiO<sub>4</sub>] surface was prepared by depositing less than 1 ML Si onto a Mo(112)–p(2 × 3)-O surface, followed by an anneal at 800 K in a  $1 \times 10^{-7}$  Torr O<sub>2</sub> for 5 min, with an increase in the temperature to 1200 K for an additional 5 min. This procedure was repeated until a constant Si/Mo AES ratio was achieved.

Benzene and pyridine (>99.0%, EM Science) were degassed using numerous freeze–thaw cycles prior to use. Exposures were determined using an ion gauge with no correction for sensitivity. Coverages were estimated using benzene adsorption on the clean Mo(112) surface,<sup>27</sup> noting the AES break point on the Mo(112)–c(2 × 2)-[SiO<sub>4</sub>] surface and assuming a unity sticking coefficient. The AES data were acquired with a primary beam energy of 2000 eV and an electron beam current of 1  $\mu$ A. To minimize electron beam effects on the adsorbed benzene layer, the AES data were acquired in as short a period as

\* To whom correspondence should be addressed. E-mail: goodman@mail.chem.tamu.edu.

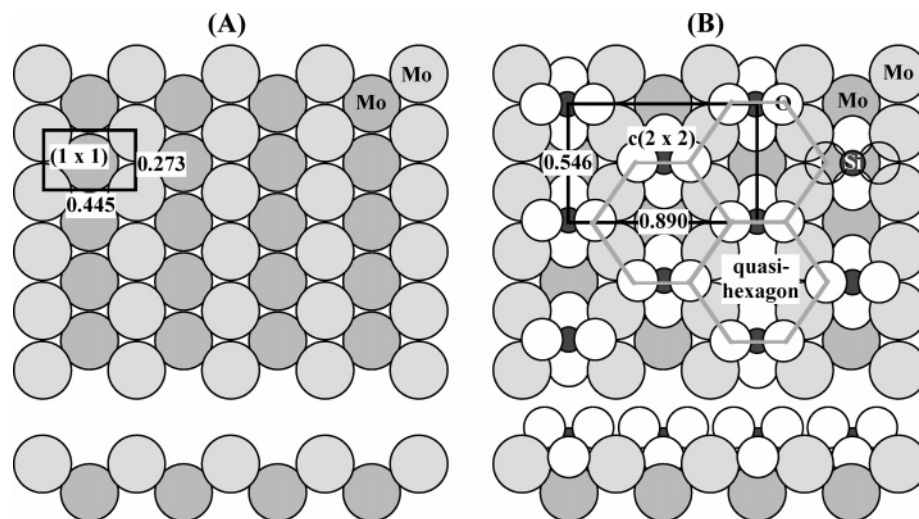


**Figure 1.** Top view and side view of (A) Mo(112) and (B) Mo(112)-c(2 × 2)-[SiO<sub>4</sub>] surface structures.<sup>23</sup>

possible. The energy resolution of the HREELS measurements was between 64 and 96 cm<sup>-1</sup> (8 ~ 12 meV) as determined by the full width at half-maximum (fwhm) of the elastic peak; the monochromatized electrons were incident at an angle of 60° with respect to the sample normal. The analyzer could be rotated about its axis for on- and/or off-specular measurements; a primary energy (E<sub>p</sub>) of ~5 eV was used.

### 3. Results

How adsorption symmetry and dipole influence the vibrational modes of benzene has been reviewed and discussed in detail by Sheppard.<sup>2</sup> Briefly, the benzene molecule, with a *D*<sub>6h</sub> point group in the gas phase, is reduced to *C*<sub>6v</sub> or lower symmetry when adsorbed with a geometry parallel to the surface. At least three modes, in-plane C–H stretching ( $\nu$ CH), ring stretching ( $\nu$ CC), and out-of-plane C–H bending ( $\gamma$ CH), are dipole allowed for a benzene molecule parallel to the surface. With lower symmetries additional modes become dipole active, for example, in-plane C–H bending ( $\delta$ CH). Note that  $\nu$ CH and  $\delta$ CH have dynamic dipole components parallel to the benzene molecular plane, while that for  $\gamma$ CH is perpendicular to the molecular plane. Hence, based on the surface dipole selection rule, the number of vibrational modes observed in the HREEL spectrum and/or the relative intensities of the  $\nu$ CH and  $\gamma$ CH modes, in principle, can be used to determine the adsorption geometries.

**3.1 Benzene Adsorbed on Mo(112)-c(2 × 2)-[SiO<sub>4</sub>].** HREELS data for benzene adsorbed at various exposures on the Mo(112)-c(2 × 2)-[SiO<sub>4</sub>] surface at 90 K are shown in Figure 2. For comparison, a spectrum of the Mo(112) surface and one of ~2 ML benzene adsorbed on the Mo(112) surface are shown in the lower panel in Figure 2.<sup>27</sup> The spectra have been normalized to the elastic peak intensities, giving rise to differences in the signal-to-noise ratio because of variations in the intensity of the elastic peak among experiments. Assignment of the HREELS modes of adsorbed benzene is made on the basis of vibrational assignments of the IR spectrum of gas-phase benzene.<sup>28</sup> Several phonon features of the substrate c(2 × 2)-[SiO<sub>4</sub>] surface are apparent at 40, 86, 96, and 131 meV (320, 688, 768, and 1048 cm<sup>-1</sup>) and have been discussed in detail.<sup>23</sup> Among these, the 86 meV (688 cm<sup>-1</sup>) feature is very near that of the C–H out-of-plane bending mode ( $\gamma$ CH) for gas-phase benzene at 674 cm<sup>-1</sup>. Upon an increase in the benzene coverage, the intensity of the phonon feature at 86 meV increases rapidly,

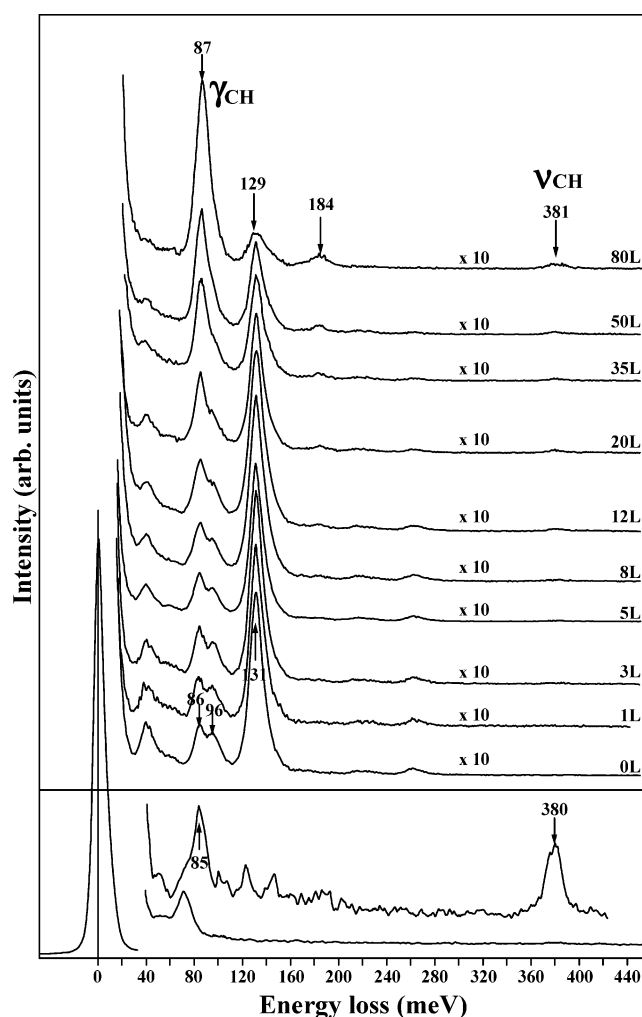


**Figure 2.** (Upper panel): Specular HREEL data for benzene on the Mo(112)-c(2 × 2)-[SiO<sub>4</sub>] surface at 90 K obtained as a function of increasing exposures. (Lower panel): A HREEL spectrum of Mo(112) and a spectrum of 2 ML benzene on Mo(112) indicating a tilted adsorption geometry that gives rise to an intense  $\nu$ CH feature at 380 meV.<sup>27</sup>

while the feature at 131 meV decreases gradually. The frequency and the increase of intensity of the 86 meV feature is consistent with it corresponding to the  $\gamma$ CH mode of benzene, while the decrease in the 131 meV band is consistent with it being

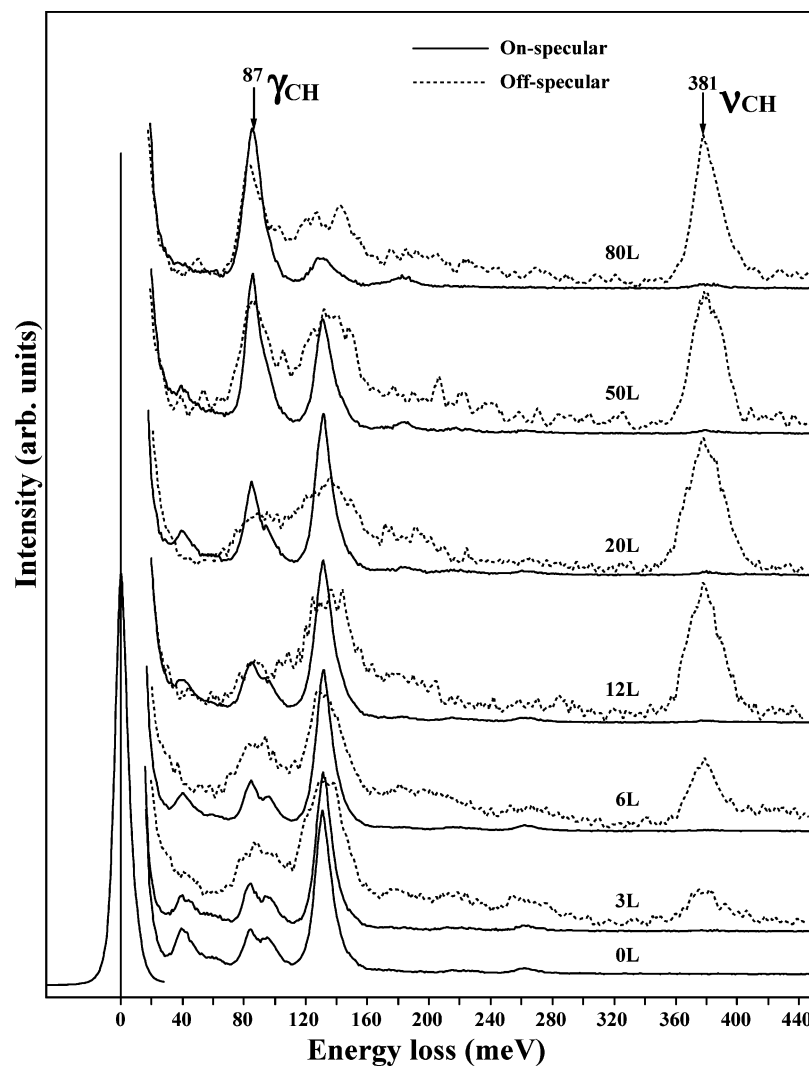


**Figure 3.** Comparison of specular and off-specular HREEL data for benzene on Mo(112)-c(2 × 2)-[SiO<sub>4</sub>] at 90 K.

assigned to the substrate phonon feature whose intensity is attenuated by the benzene overlayer. It has been shown that the  $\gamma$ CH mode is sensitive to the nature of the adsorption site and bonding strength.<sup>29</sup> The value of 86 meV (688 cm<sup>-1</sup>) is very near 673 cm<sup>-1</sup> for gas phase benzene, indicating that molecular benzene is bonded weakly to the Mo(112)-c(2 × 2)-[SiO<sub>4</sub>] surface. This observation is consistent with a  $\gamma$ CH mode at 690 cm<sup>-1</sup> obtained on the oxygen-modified Mo(110) surfaces where the interaction between benzene and the surface is relatively weak deduced from temperature-programmed desorption that is weaker than on the clean Mo(110) surface with a  $\gamma$ CH mode at 704 cm<sup>-1</sup>.<sup>30</sup> For submonolayer to multilayer (~13 ML) benzene exposures, no significant features corresponding to the C-H in-plane stretching mode ( $\nu$ CH) at 375 ~ 385 meV (3000 ~ 3080 cm<sup>-1</sup>) are apparent in the specular data. At high exposures, two new bands, corresponding to the C-H in-plane bending ( $\delta$ CH) and ring-stretching ( $\nu$ CC) modes, appear at ~129 meV (1032 cm<sup>-1</sup>) and ~184 meV (1472 cm<sup>-1</sup>), respectively. Off-specular data for various benzene exposures were acquired and are compared with the specular data in Figure 3. The off-specular data show significant intensity at ~381 meV (3048 cm<sup>-1</sup>) corresponding to the  $\nu$ CH mode. Compared with the specular data, the relative peak intensities of the  $\gamma$ CH and  $\nu$ CH features are markedly different. Such strong angular dependence of the intensities for the  $\gamma$ CH and  $\nu$ CH modes<sup>31</sup> suggests, on the basis of the surface dipole selection rule, that

benzene is bonded with its molecular plane parallel or nearly parallel to the surface plane, or it forms a crystalline phase as reported for polycrystalline platinum.<sup>32</sup>

**3.2 Pyridine Adsorption on Mo(112)-c(2 × 2)-[SiO<sub>4</sub>].** To better understand the adsorption geometry and coverage of benzene, pyridine adsorption on the c(2 × 2)-[SiO<sub>4</sub>] surface was also investigated. The orientation of pyridine changes from a parallel to a tilted configuration as the coverage is increased from one to two monolayers. As shown in Figure 4, no obvious  $\nu$ CH band below 5 L is apparent, while the  $\nu$ CH band at 382 meV (3056 cm<sup>-1</sup>) appears above an exposure of 7 L and rapidly increases in intensity with increasing pyridine exposure. These results are consistent with the 6 L exposure corresponding to a monolayer coverage, as seen for benzene on Mo(112).<sup>27</sup>

## 4. Discussion

**4.1. Orientation of Benzene on Mo(112)-c(2 × 2)-[SiO<sub>4</sub>].** On the oxide surfaces MgO,<sup>13</sup> TiO<sub>2</sub>,<sup>14-16</sup> and ZnO,<sup>17,18</sup> benzene adsorbs with its plane parallel to the surface and its  $\pi$  electrons interacting with the oxide cations. A proposed structure of the c(2 × 2)-[SiO<sub>4</sub>] surface places the oxygen atoms in the outmost layer, for example, O-terminated, as shown in Figure 1B.<sup>23</sup> For benzene adsorption on this surface, there is no possibility for direct interaction of the benzene with the Si<sup>4+</sup> cations. Consequently, a weak electrostatic interaction is anticipated between

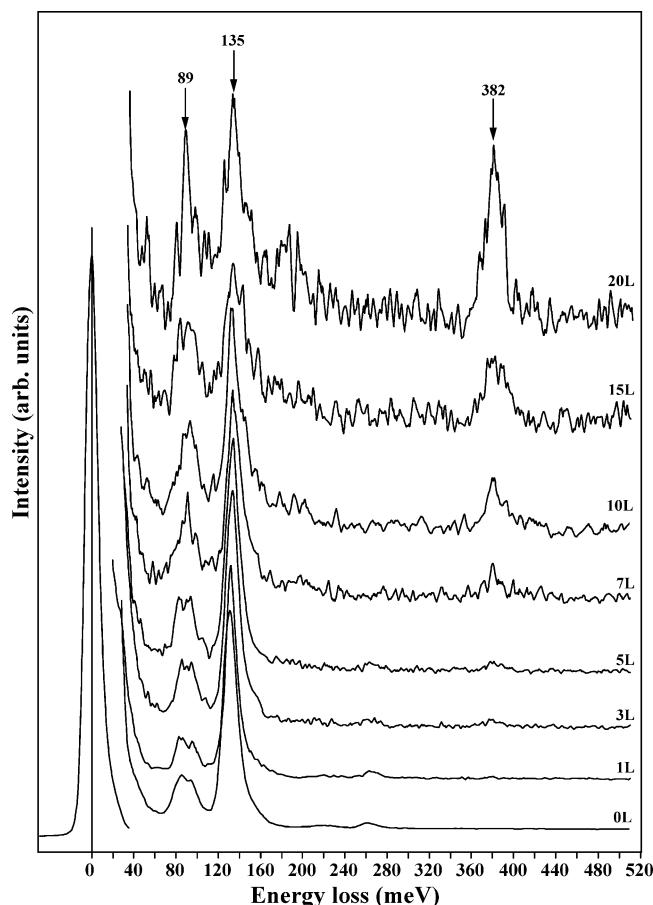


**Figure 4.** Specular HREEL data for pyridine on Mo(112)- $c(2 \times 2)$ -[SiO<sub>4</sub>] at 90 K as a function of increasing exposure.

the hydrogens of benzene and the top layer oxygen anions in the  $c(2 \times 2)$ -[SiO<sub>4</sub>] surface. TPD shows that benzene desorbs from the surface below 160 K, consistent with a weak interaction. On an O-terminated oxide surface, SiO<sub>2</sub>/Mo(112),<sup>33</sup> TiO<sub>2</sub>(100)-(1 × 3)<sup>34</sup> and on TiO<sub>2</sub>(110),<sup>15</sup> benzene adopts a tilted adsorption geometry. However, on the  $c(2 \times 2)$ -[SiO<sub>4</sub>] surface, as shown in Figure 2, there is no evidence of a tilted configuration ( $\nu$ CH in the specular data) over the entire range of coverages (from submonolayer to 80 L (~13 ML)). Only a parallel adsorption geometry or formation of crystalline benzene can produce the observed spectra (*c.f.* Figures 2 and 3). To clarify the nature of the benzene adsorption at submonolayer coverages, off-specular data were collected for 3 and 6 L (~0.5 and 1 ML exposures, respectively) of benzene (Figure 3). In the off-specular data, the  $\nu$ CH feature at 380 meV (3040 cm<sup>-1</sup>) is well resolved and intense. The formation of a 3-D crystalline island should result in a relatively low cross-section for this feature since a monolayer would cover only a relatively small part of the surface. The intensity of the  $\nu$ CH feature in the off-specular data, in turn, would be low. Thus, we conclude that benzene adopts a parallel geometry on the  $c(2 \times 2)$ -[SiO<sub>4</sub>] within the first layer. Furthermore, heating a 50 L sample to ~150 K, which removes multilayer benzene, yields a HREEL spectrum in which the residual  $\gamma$ CH band intensity is very near that for one monolayer of benzene. These data are consistent with the benzene covering the entire surface rather than forming 3-D crystalline islands at less than 1 ML coverage.

The  $c(2 \times 2)$ -[SiO<sub>4</sub>] surface structure is assumed to be that of Figure 1B,<sup>23</sup> where the outmost layer oxygen atoms are arranged in a quasi-hexagonal configuration. Assuming a trans-hydrogen separation in benzene of 0.494 nm, a  $c(2 \times 2)$

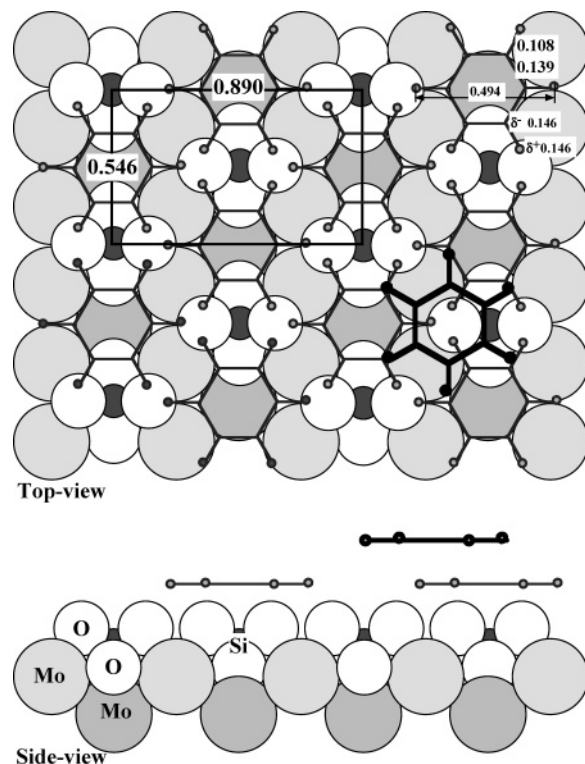


**Figure 5.** Top and side view of the possible adsorption sites and orientation for parallel bonded benzene on Mo(112)- $c(2 \times 2)$ -[SiO<sub>4</sub>]. A schematic of benzene is shown as a thin line in the first layer and as a thicker line in the second layer.

structure, as shown in Figure 5, is possible in which the six hydrogen atoms in each benzene molecule interact with the oxygen atoms via electrostatic interactions. The LEED data indicate a  $c(2 \times 2)$  pattern at <2–3 ML, consistent with this structure. However, the Mo(112)- $c(2 \times 2)$  unit size of 0.546 nm is less than the van der Waals diameter (0.65 nm) of benzene.<sup>35</sup> In the proposed geometry, the repulsive force between positively charged hydrogen atoms may be partially screened by the interaction with negatively charged oxygen atoms as illustrated in Figure 5, making the parallel geometry more stable than the tilted one in which only two of the six hydrogen atoms interact with the substrate oxygen atoms. Note that in the bulk crystal, benzene molecules are located in a “T-shaped” configuration with respect to each other where the nearest molecular center-to-center distance is 0.498 nm.<sup>1</sup> This benzene geometry is stabilized by the fact that all six positively charged H atoms in each molecule interact with the neighboring negatively charged carbon rings.

#### 4.2 Growth Mode of Benzene on Mo(112)- $c(2 \times 2)$ -[SiO<sub>4</sub>].

To further elucidate the benzene geometry and growth mode on the  $c(2 \times 2)$ -[SiO<sub>4</sub>] surface, AES was used to measure the C/Mo ratios as a function of benzene coverage. To reduce the effects of electron beam damage in the benzene overlayer, an Auger beam current of 1  $\mu$ A (2 keV) was used and each AES spectrum was acquired within 10 s. Figure 6A shows AES spectra measured for several benzene exposures. The increasing intensity of the C(271) feature correlates with an increase in the benzene coverage. The bottom spectrum in Figure 6A, obtained after heating the sample to ~160 K to desorb benzene, indicates no residual carbon signal and is consistent with no appreciable thermal or electron beam decomposition. The related intensities of C(271) relative to Mo(186), for example, the C/Mo AES ratio, versus benzene exposures are shown in Figure 6B. For comparison, the C/Mo AES ratio versus pyridine exposures



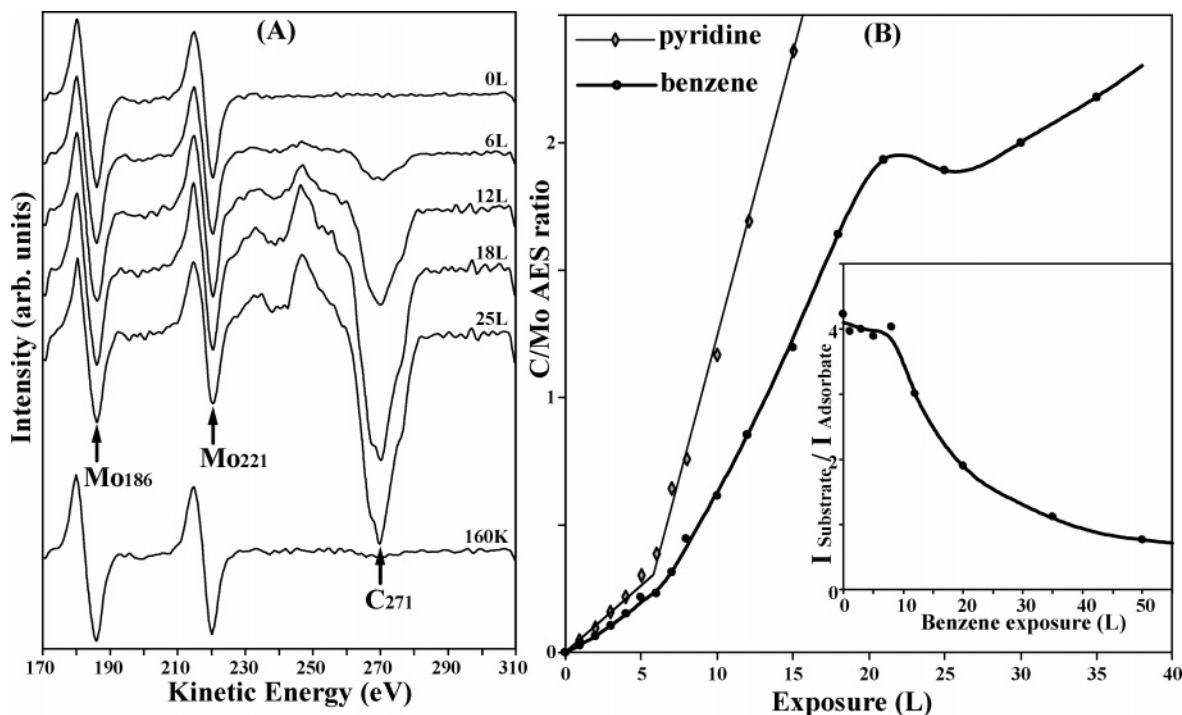


**Figure 6.** (A) AES spectra of benzene on Mo(112)- $c(2 \times 2)$ -[SiO<sub>4</sub>] at 90 K as a function of exposure. The bottom spectrum was obtained by annealing a surface covered with a 35 L benzene exposure at 160 K and after approximately 16 AES measurements. (B) Plots of C(271)/Mo(186) AES ratio versus benzene (or pyridine) exposures on Mo(112)- $c(2 \times 2)$ -[SiO<sub>4</sub>]. The insert is a plot of the ratio of the phonon peak intensity at 131 meV divided by that at 86 meV versus benzene exposure on the  $c(2 \times 2)$ -[SiO<sub>4</sub>] surface.

are also displayed. The benzene and pyridine data indicate a break point in the C/Mo ratio versus coverage plots at  $\sim 6$  L, with a linear relationship of the data before and after the break point. The slope of the plots after the break point is obviously greater than that prior to the break point, consistent with a layer-by-layer growth mode (Frank–van der Merwe model).<sup>36,37</sup> Since pyridine adsorbed on the  $c(2 \times 2)$ -[SiO<sub>4</sub>] surface exhibits a phase change from a parallel to tilted geometry at a pyridine exposure between 5  $\sim$  7 L (*cf.* section 3.2 and Figure 4), the similarity of the growth parameters between benzene and pyridine support the assumed benzene coverage and growth mode. In contrast to pyridine, a second break point was observed after a 20 L benzene exposure with a subsequent reduction in the slope of the C/Mo versus coverage plot. The origin of this second break point is not clear but may be due to a phase change or an altered growth mode. The HREEL spectra (*cf.* Figure 2) show no obvious  $\nu$ CH features over the entire benzene coverage range, therefore the break point after 20 L exposure likely relates to the formation of 3-D crystalline clusters.

A careful inspection of the HREEL spectra for benzene on the  $c(2 \times 2)$ -[SiO<sub>4</sub>] surface (*cf.* Figure 2), shows that the substrate Si–O stretching phonon feature at 131 meV, rather than the 86 eV feature, is attenuated by the benzene overlayer. The intensity of the 86 eV feature, in fact, increases with increasing benzene exposure. The 131 meV feature corresponds to an oxide phonon mode, and the 86 meV to the C–H mode of parallel bonded benzene and/or benzene in the crystalline phase. Their relative intensities, for example, the ratio of intensities of the 131 to the 86 meV features ( $I_{\text{substrate}}/I_{\text{adsorbate}}$ ), can be used as an attenuation index, characteristic of the growth mode. A plot of this ratio versus benzene exposure, inserted into Figure 6B, shows a relatively slow rate of change within the submonolayer regime with a sharply increasing rate of change at intermediate coverages; a reduction in slope occurs at the highest exposures. This behavior suggests layer-by-layer

growth at low exposure followed by 3-D cluster formation at higher exposures, consistent with the AES results.

From the above results and discussion, the initial formation of a crystalline benzene phase at submonolayer coverages can be excluded. Furthermore, the absence of an obvious  $\nu$ CH feature in the HREELS data clearly shows that the parallel geometry is adopted in the first, second, and third layers. Recent results<sup>38</sup> for benzene adsorption on Mo(112)- $(8 \times 2)$ -TiO<sub>x</sub> indicates layer-by-layer growth with a tilted geometry up to  $\sim 6$  ML before 3-D crystallization, whereas for benzene on Mo(112)- $(2 \times 3)$ -(TiO<sub>x</sub>-[SiO<sub>4</sub>]), parallel and tilted geometries coexist in the first layer with subsequent 3-D crystallization.

On metal surfaces,<sup>2,3</sup> the consensus is that benzene adsorbs with its molecular plane parallel to the surface, with the  $\pi$  electrons of the benzene ring interacting with the metal surface. Subsequent layers adopt a tilted geometry, ultimately forming a 3-D crystalline phase. On a weakly interacting surface, for example, graphite, the first monolayer of benzene bonds parallel to the surface, with subsequent formation of a crystalline phase.<sup>39–41</sup> On the Mo(112)- $c(2 \times 2)$ -[SiO<sub>4</sub>] surface, a  $c(2 \times 2)$  unit is formed similar to that discussed in section 4.1 (*cf.* Figure 5). Accordingly, benzene, located within each  $c(2 \times 2)$  unit, bonds electrostatically to the substrate oxygen atoms via the six hydrogen atoms. Likewise, the second layer of benzene positions itself within the  $c(2 \times 2)$  unit cell with its molecular plane parallel to the surface. By rotating the benzene molecule 90° and translating it one-half the molecular diameter with respect to the first layer benzene, the second layer benzene can occupy a site such that the carbon ring is located directly above the three hydrogen atoms of the first layer benzene, with each hydrogen atom located above the first layer benzene ring. This geometry is stabilizing in that the six hydrogen atoms of each benzene molecule in the second layer can interact with the aromatic benzene rings of the first layer, similar to the intermolecular interactions in crystalline benzene.<sup>1</sup>

## 5. Conclusions

Benzene adsorbs on the well-ordered Mo(112)-c(2 × 2)-[SiO<sub>4</sub>] surface with its molecular plane parallel to the surface plane in the initial layer, where all six hydrogen atoms in each benzene molecule bond electrostatically to the surface oxygen anions. From AES data and attenuation of the HREELS features, a layer-by-layer growth model is confirmed for the initial three layers; subsequent benzene exposure forms a 3-D crystalline phase. Since the νCH mode exhibits no apparent intensity over the entire benzene exposure range (<10 ML), the benzene molecules within the first three layers are oriented parallel to the surface. Due to a close match between the substrate lattice and the benzene dimensions, this layer-by-layer, parallel packing facilitates attractive electrostatic interactions between the hydrogen atoms and the aromatic rings of adjacent benzene layers. Pyridine on the c(2 × 2)-[SiO<sub>4</sub>] surface, on the other hand, changes from a parallel bonded configuration to a tilted one within the first monolayer.

**Acknowledgment.** We acknowledge with pleasure the support of this work by the Department of Energy, Office of Basic Energy Sciences, Division of Chemical Sciences, the Robert A. Welch Foundation, U. S. Civilian Research & Development Foundation, and the Texas Advanced Technology Program under Grant No. 010366-0022-2001.

## References and Notes

- (1) Cox, E. G. *Rev. Modern Phys.* **1958**, *30*, 159.
- (2) Steppard, N. *Annu. Rev. Phys. Chem.* **1988**, *39*, 589.
- (3) Netzer, F. P. *Langmuir* **1991**, *7*, 2544.
- (4) Haq, S.; King, D. A. *J. Phys. Chem.* **1996**, *100*, 16957.
- (5) Syomin, D.; Kim, J.; Koel, B. E. *J. Phys. Chem. B* **2001**, *105*, 8387.
- (6) Netzer, F. P.; Rangelov, G.; Rosina, G.; Saalfeld, H. B.; Neumann, M.; Lloyd, D. R. *Phys. Rev. B* **1988**, *37*, 10399.
- (7) Fujisawa, M.; Sekitani, T.; Morikawa, Y.; Nishijima, M. *J. Phys. Chem.* **1991**, *95*, 7415.
- (8) Eng, J., Jr.; Chen, J. G.; Abdelrehim, I. M.; Madey, T. E. *J. Phys. Chem. B* **1998**, *102*, 9687.
- (9) Henrich, V. E.; Cox, P. A. *The Surface Science of Metal Oxides*; Cambridge University Press: Cambridge, 1994.
- (10) Freund, H. J. *Surf. Sci.* **2002**, *500*, 271.
- (11) Goodman, D. W. *J. Catal.* **2003**, *216*, 213.
- (12) Santra, A. K.; Goodman, D. W. *J. Phys. C* **2002**, *12*, R31.
- (13) Street, S. C.; Guo, Q.; Xu, C.; Goodman, D. W. *J. Phys. Chem.* **1996**, *100*, 17599.
- (14) (a) Nagao, M.; Suda, Y. *Langmuir* **1989**, *5*, 42. (b) Boddenberg, B.; Eltzner, K. *Langmuir* **1991**, *7*, 1498.
- (15) Reiss, S.; Krumm, H.; Niklewski, A.; Staemmler, V.; Wöll, Ch. *J. Chem. Phys.* **2002**, *116*, 7704.
- (16) Raza, H.; Wincott, P. L.; Thornton, G.; Casanova, R.; Rodriguez, A. *Surf. Sci.* **1998**, *402–404*, 710.
- (17) Sosa, A. G.; Evans, T. M.; Parker, S. C.; Campbell, C. T.; Thornton, G. *J. Phys. Chem. B* **2001**, *105*, 3783.
- (18) Rubloff, G. W.; Lüth, H.; Grobman, W. D. *Chem. Phys. Lett.* **1976**, *39*, 493.
- (19) Goodman, D. W. *Surf. Rev. Lett.* **1995**, *2*, 9.
- (20) Campbell, C. T. *Surf. Sci. Rep.* **1997**, *27*, 1.
- (21) Franchy, R. *Surf. Sci. Rep.* **2000**, *38*, 195.
- (22) Chambers, S. A. *Surf. Sci. Rep.* **2000**, *39*, 105.
- (23) Chen, M.-S.; Santra, A. K.; Goodman, D. W. *Phys. Rev. B* **2004**, *69*, 155404.
- (24) Scott, J. F.; Porto, S. P. S. *Phys. Rev.* **1967**, *161*, 903.
- (25) Handke, M.; Mozgawa, W. *Vib. Spectrosc.* **1993**, *5*, 75.
- (26) Cornac, M.; Janin, A.; Lavalley, J. C. *Polyhedron* **1986**, *5*, 183; *Infrared Phys.* **1984**, *24*, 143.
- (27) Chen, M.-S.; Goodman, D. W., unpublished. Benzene adsorbs molecularly on Mo(112) with its molecular plane parallel to the surface at submonolayer coverages. With further increase in the benzene coverage, a tilted geometry is adopted, giving rise to a prominent C–H in-plane stretching mode at 380 meV. A shift of the geometry from parallel to tilted at ~6 L was used to estimate the benzene coverage by assuming a unity sticking coefficient.
- (28) Dang-Nhu, M.; Pliva, J. *J. Mol. Spectrosc.* **1989**, *138*, 423.
- (29) Koel, B. E.; Crowell, J. E.; Mate, C. M.; Somorjai, G. A. *J. Phys. Chem.* **1984**, *88*, 1988.
- (30) Eng, J., Jr.; Bent, B. E.; Frühberger, B.; Chen, J. G. *J. Phys. Chem. B* **1997**, *101*, 4044.
- (31) Netzer, F. P.; Ramsey, M. G. *Cri. Rev. Solid State Mater. Sci.* **1992**, *17*, 397.
- (32) Swiderek, P.; Winterling, H. *Chem. Phys.* **1998**, *229*, 295.
- (33) Chen, M.-S.; Goodman, D. W., unpublished. On a thick SiO<sub>2</sub> film grown on the Mo(112) surface, benzene adsorbs with a tilted geometry from submonolayer to multilayer coverages.
- (34) Landree, E.; Marks, L. D.; Zschack, P.; Gilmore, C. J. *Surf. Sci.* **1998**, *408*, 300.
- (35) Williams, D. E.; Xiao, Y.-L. *Acta Crystallogr.* **1993**, *A49*, 1.
- (36) Frank, F. C.; van der Merwe, J. H. *Proc. R. Soc. London Ser. A* **1949**, *198*, 205.
- (37) Argile, C.; Rhead, G. E. *Surf. Sci. Rep.* **1989**, *10*, 277.
- (38) Chen, M.-S.; Goodman, D. W., unpublished.
- (39) Cameson, I.; Rayment, T. *Chem. Phys. Lett.* **1986**, *123*, 150.
- (40) Meehan, P.; Rayment, T.; Thomas, R. K.; Bomchil, G.; White, J. *W. J. Chem. Soc., Faraday Trans. 1* **1980**, *76*, 2011.
- (41) Bardi, U.; Magnanelli, S.; Rovida, G. *Langmuir* **1987**, *3*, 159.